

NUMERICAL SIMULATION OF TURBULENT FLOW
THROUGH TANDEM CASCADE

Diao Xu and Guo-chuan Wu
Power Engineering Department
Nanjing Aeronautical Institute
Nanjing Jiangsu, The P.R.C.

Abstract

Turbulent flows through single and tandem cascades of airfoil are numerical simulated using finite analytic numerical method. The $k-\epsilon$ turbulent model and wall-function approach are utilized to describe turbulent flow process and wall-proximity region in the numerical simulations. In order to solve more practical engineering problem, the body-fitted coordinate transformation is incorporated in the finite analytic method in the present study. The finite analytic method is firstly introduced into the numerical calculations of cascade flow fields. In the present study, the excellent agreement with other's solutions and experiment data is obtained.

I. Introduction

Now, the tandem cascade of airfoil has been used on stators and rotors in some fans and compressors of aero-engines, in inducers and diffusers of high-pressure centrifugal compressors.[1,2] It seems to be one of hopeful way to raise stage load and enlarge the range of stable operation.

There have been several researchers studied the flow fields through the tandem cascade of airfoil using various numerical methods, such as, Spralin[3] (1951), Mikolajczak [4] (1970), Sanger [5] (1971), and Bammert [6] (1980). But, as its geometrical complicity, the turbulent flow fields through tandem cascade of airfoil has never been studied numerically until now.

A recently developed finite analytic method (FA) is adopted in the present study to study the incompressible, steady and turbulent flow through the single and tandem cascades of airfoil in general curvilinear coordinates. The basic idea of the FA is to invoke the analytic solution of governing partial differential equation in the numerical solution of the problem. In the FA method, the total calculating region of problem is divided into a number of small subregions in which the governing equation, if nonlinear, such as the Navier-Stokes equation is locally linearized. The local analytic solution is then expressed in an algebraic form, relating an interior nodal value of the subregion to its neighboring nodal values. The system of the algebraic equations derived from

the local analytic solution is then solved to provide the numerical solution of the total problem.[7]

At present, there are many numerical approaches to deal with the Navier-Stokes equations, such as the finite difference (FD) method and finite element (FE) method. Many successful application of FD method in turbulent flow field calculations have been obtained[8]. But, with FD method, the instability of solution of difference equations is often encountered when the character of the partial differential equation is not properly considered. An error known as "numerical diffusion" may result when the nonlinear or quasi-linear term in partial differential equation is not approximated[9]. FE method is also widely used in the numerical calculations of the Navier-Stokes equations. Instability also occurs in solving the system of algebraic equations derived from the FE method at high Reynolds number flow [10].

The FA method, developed by Chen et al. [7,11], is adopted in the present study to solve the turbulent flow through single and tandem cascades of airfoil. As the FA solution is derived from local linearized analysis of partial differential equations, it has good accurate, and also due to its analytic nature of solution, it builds in automatically upwind shifting of influence for the neighboring nodals on the solution. As Chen said, the stability of the algebraic equation derived from the FA method is quite good.

Although the general principle of the present study follows the original idea of Chen, the present study suffers severely from geometric limitation since in the original work of Chen the Navier-Stokes equations were written in Cartesian or cylindrical polar coordinates and the numerical calculating was only done in such coordinates. Application of FA method to curved surface such as the single and tandem cascades of airfoil must involve interpolation between grid points not coincide with the boundaries. This may adversely affect the accuracy of the solutions. In the present study, this geometric limitation is removed by adopting a general curvilinear coordinate system. Thus the FA method is introduced into the numerical solutions of single and tandem cascades of airfoil in the general curvilinear coordinates.

At present, one can not solve the N-S equations directly as the limitation of computer storage. The time-averaged N-S equations and k-ε turbulent model has been used in the present study. The wall function method is also employed to deal with the wall-proximity region and boundary conditions on solid surface.

The numerical simulation of flow through a single cascade of airfoil is very important in the aerodynamic design of turbomachinery components. As a testment, the turbulent flow through a single cascade of NACA65 airfoil was simulated using the FA method in the body-fitted coordinate system. The numerical results compared with the experimental data show excellent agreement. The turbulent flow through a tandem cascade of airfoil, then, was calculated using the same method. The numerical results compared with the authors' experimental data is quite good.

II. Numerical Method

Governing Equations

The present study is based on the numerical solution of two-dimensional form of the time-averaged continuity, N-S and high Reynolds number k-ε turbulent equations. With this approach, the equations for the present study can be written in the general form in Cartesian coordinate

$$\begin{aligned} & \partial(\rho U \phi) / \partial x + \partial(\rho V \phi) / \partial y = \\ & \partial(\Gamma_{\phi} \partial \phi / \partial x) / \partial x + \partial(\Gamma_{\phi} \partial \phi / \partial y) / \partial y \\ & + S_{\phi} \end{aligned} \quad (1)$$

where ϕ stands for different dependent variables for which the equations are to be solved. The equations used in the present study are summarized in the Tab.1

Tab.1 Summary of Governing Equations

Equation	ϕ	Γ_{ϕ}	S_{ϕ}
Continuity	1	0	0
X-momentum	U	$\mu + \mu_t$	$-\partial p / \partial x + \partial(\mu_{xy} \partial U / \partial x) / \partial x + \partial(\mu_{xy} \partial V / \partial y) / \partial y - 2\rho k / 3$
Y-momentum	V	$\mu + \mu_t$	$-\partial p / \partial y + \partial(\mu_{xy} \partial U / \partial y) / \partial x + \partial(\mu_{xy} \partial V / \partial y) / \partial y - 2\rho k / 3$
Turbulence energy	k	$\mu + \frac{\mu_t}{\sigma_k}$	$\rho P - \rho \epsilon$
Energy dissipation	ε	$\mu + \frac{\mu_t}{\sigma_{\epsilon}}$	$C_1 \rho \epsilon P / k - C_2 \rho \epsilon^2 / k$

where $\mu_t = C_{\mu} \rho k^2 / \epsilon$
and $P = \frac{1}{2} (2((\partial U / \partial x)^2 + (\partial V / \partial y)^2) + ((\partial U / \partial y) + (\partial V / \partial x))^2)$
and the constants are

C_{μ}	C_1	C_2	σ_k	σ_{ϵ}
0.09	1.45	1.90	1.0	1.3

The turbulence scalar transport equations are only valid for full developed turbulent region. An additional model must be introduced to treat the laminar sublayer region on the wall-proximity region. The wall function method was used in the present study to treat wall-proximity region and to eliminate the large number of grid points needed to resolve the laminar sublayer region. The wall function is given as

$$\begin{cases} u^+ = \frac{1}{K} \ln(E \cdot y^+) & 120 > y^+ > 12 \\ v = 0 \end{cases} \quad (2)$$

$$\begin{cases} u^+ = y^+ & 12 > y^+ > 0 \\ v = 0 \end{cases} \quad (3)$$

where $u^+ = u / u_{\tau}$, $y^+ = y \cdot u_{\tau} / \nu$
where u_{τ} is the friction velocity and $u_{\tau}^2 = \tau_w / (\rho U^2)$, τ_w is the wall shear stress. E and K are constants.

In order to solve more practical engineering problem, the body-fitted coordinate transformation was incorporated in the present study.

$$\begin{aligned} \xi &= \xi(x, y) \\ \eta &= \eta(x, y) \end{aligned} \quad (4)$$

When new independent variables ξ and η are introduced, the form of the governing equations will be changed as follow

$$2A_{\phi} \phi_{\xi}^2 + 2B_{\phi} \phi_{\eta}^2 = C_{\phi} \phi_{\xi\xi} + D_{\phi} \phi_{\eta\eta} + G_{\phi} \quad (5)$$

where coefficients A, B, C and D are generated by coordinates transferring. G is regarded as source term.

The source term in Eq.5 can be eliminated by further assuming that

$$\phi' = \phi - (A\xi + B\eta) \cdot C_{\phi} / (2(A^2 + B^2)) \quad (6)$$

Then

$$2A_{\phi} \phi_{\xi}^{\prime 2} + 2B_{\phi} \phi_{\eta}^{\prime 2} = C_{\phi} \phi_{\xi\xi}^{\prime} + D_{\phi} \phi_{\eta\eta}^{\prime} \quad (7)$$

Finite Analytic Method

The basic idea of the finite analytic method is to incorporate analytic solution in the numerical solution of linear or nonlinear partial differential equations. In the FA method, the whole calculating region of the problem is divided into a number of small elements in which the governing equation is solved analytically. An algebraic equation which approximates the governing equation is then obtained for numerical solution.

In term of the notation shown in Fig.2 for a typical grid nodal P enclosed in its cell and surrounded by its neighboring NC, SC, WC, EC, NE, NW, SE and SW, an analytic solution of governing equation can be obtained in the element due to its simple geometry. However, if the governing equation is nonlinear, such as the Navier-Stokes equation, the equation may be locally linearized in the element so that an analytic solution can be obtained. In this fashion, the overall non-

linear effect can still be approximately preserved by assembly of local linearized analytic solutions which constitute the numerical solution of partial differential equation over the whole calculating region of the problem.

In order to derive an analytic solution in an element, as shown in Fig.2, the Eq.7 is linearized, i.e. the coefficients in Eq.7 are assumed to be constants in the element. The central node P is surrounded by its four boundaries (east, west, north and south). The ellipticity of Eq.7 in space requires that the four boundary conditions ϕ_N , ϕ_E , ϕ_S , and ϕ_W be specified. We choose the approximate functions from class functions which satisfy the governing equation to approximate the boundary conditions where three nodal values are available for each boundary. For example, the north boundary condition is approximated by

$$\phi'_N(\xi) = a_N(\exp(2A\xi/C) - 1) + b_N\xi^2 + c_N \quad (8)$$

where

$$a_N = (\phi'_{NW} + \phi'_{NE} - 2\phi'_{NC}) / (4\sinh(Ah/C))$$

$$b_N = (\phi'_{NW} + \phi'_{NE} - \coth(Ah/C) (\phi'_{NW} + \phi'_{NE} - 2\phi'_{NC})) / 2h$$

$$c_N = \phi'_{NC} \quad (9)$$

The boundary conditions for south, west and east sides can be similarly approximated as north side. With the coefficients in Eq.7 considered to be constants in an element, a simple analytic solution can be obtained for Eq.7 by method of separation of variables when proper boundary condition is specified. The local analytic solution, when evaluated at the center node P of the element, gives the FA algebraic equation relating central nodal values ϕ'_P and its eight neighboring nodal values as

$$\phi'_P = C_{EC}\phi'_{EC} + C_{WC}\phi'_{WC} + C_{NC}\phi'_{NC} + C_{SC}\phi'_{SC} + C_{NW}\phi'_{NW} + C_{SE}\phi'_{SE} + C_{SW}\phi'_{SW} + C_{WE}\phi'_{WE} \quad (10)$$

Substitute relation Eq.6 into Eq.10, we get the FA algebraic equation

$$\phi'_P = C_{EC}\phi_{EC} + C_{WC}\phi_{WC} + C_{NC}\phi_{NC} + C_{SC}\phi_{SC} + C_{NW}\phi_{NW} + C_{SE}\phi_{SE} + C_{SW}\phi_{SW} + C_{WE}\phi_{WE} + C_p g \quad (11)$$

where

$$C_p = (Ah (C_{NW} + C_{SW} + C_{WE} - C_{SE} - C_{EC} - C_{SC})) + Bk (C_{SE} + C_{NW} + C_{SC} - C_{WE} - C_{SW} - C_{EC}) / 2(A^2 + B^2)$$

$$g = G - h_c \quad (12)$$

The FA coefficient C's are given in the appendix. These coefficients in general are the function of A, B, C, D, h and k. They are tabulated for various values of A, B, C, D, h and k and stored in the computer for later use.

Although the overall solution procedure is similar to that of the SIMPLE procedure [8], we employed an ordinary grid system because of simplicity, instead of the staggered grid system suggested by Patankar. In the FA method, the algebraic equation is developed from nine points scheme, no pressure oscillation occurred [14].

Generation of Coordinate System

The grid generation scheme developed by

Sorenson and Steger [12] is adopted in the present study. In the scheme, the body-fitted coordinates are generated by solving the elliptic equations

$$\begin{aligned} \alpha X_{\eta\eta} - 2\beta X_{\eta\zeta} + \gamma X_{\zeta\zeta} &= 0 \\ \alpha Y_{\eta\eta} - 2\beta Y_{\eta\zeta} + \gamma Y_{\zeta\zeta} &= 0 \end{aligned} \quad (13)$$

After the grid is constructed, a simple exponential stretching technique is used to cluster the points near the solid surface. This is done in order to resolve the high gradient flow within the boundary layer. The resulting grid system is illustrated in Fig.3.

III. Results and Discussion

Turbulent Flow through Single Cascade

The objective of the present study is the investigation of the turbulent flow through the tandem cascade of airfoil, and comparison of the computed results with the experimental data. As a testment, the turbulent flow through the single cascade of NACA65 airfoil is simulated firstly because the surface pressure data of such cascade is available [13]. We calculated only the case of the single cascade of NACA65 airfoil at 13.1° incidence. The Reynolds number based on chord and upstream condition is 2.8×10^5 . The upstream turbulent kinetic energy is assumed to be 0.4%. The grid system is shown in Fig.3(a). A 51x19 grid points are used. The front and rear boundaries are located 1.0 and 1.5 chord length respectively. For inlet boundary condition, the velocity, turbulent kinetic energy and turbulent energy dissipation rate are given and for outlet boundary condition, the velocity components and the turbulent scalars are extrapolated from the inner solution by assuming that the first derivatives of flow properties along $\eta = \text{const}$

lines vanish. The velocity profile normal to the exit plane is then adjusted to satisfy the principle of the global conservation of mass.

The calculation was carried out in the transformed calculating plane, and the convergence was obtained from initial start in about 60 iterations with the convergence being determined by checking the flow field residual less than 3.0×10^{-3} . The calculation for single cascade of airfoil required about 27 minutes of IBM4341 CPU time.

The comparison between measured data and predicted result for surface pressure distribution are given in Fig.4. The surface pressure coefficient is defined as

$$C_p = (p - p_\infty) / (\rho V_\infty^2 / 2) \quad (14)$$

where reference values are taken at upstream boundary. As can be seen, the agreement is excellent. Only slight discrepancies are shown near leading and trailing edge.

Turbulent Flow through Tandem Cascade

As the method and the procedure developed by authors have been proven, the pre-

sent work is to calculate the turbulent flow through the tandem cascade of airfoil and comparison of the calculated result with the experimental data. We calculated three cases of the tandem cascade of airfoil at incidence angle of 10° , 0° and -10° respectively. The Reynolds number based on the front chord and upstream condition is 2.0×10^6 . The upstream turbulent kinetic energy is given as measured value 0.4%. The grid system is shown in Fig.3(b). A 69×21 grid points are used. The front and rear boundaries are located at 1.0 and 2.0 front chord length respectively. For inlet boundary condition, the velocity, turbulent kinetic energy and turbulent energy dissipation rate are given and for outlet boundary condition, the velocity components and the turbulent scalars are extrapolated from the inner solution by assuming that the first derivatives of flow properties along $y = \text{constant}$ lines vanish. The velocity normal to the exit plane is then adjusted to satisfy the principle of the global conservation of mass.

The calculation was carried out in the transformed calculating plane, and the convergence was obtained from initial start in about 80 iterations with convergence being determined by checking the flow field residual less than 1.0×10^{-5} . The calculation for tandem cascade of airfoil required about 30 minutes of IBM4341 CPU time.

The comparison between measured data and predicted results for surface pressure distribution are given in Fig.5. The surface pressure coefficient is defined as

$$C_p = (p - p_2) / (\rho V^2 / 2) \quad (15)$$

where reference values are taken at up and down stream boundaries respectively. As can be seen, the agreement is quite good. Only slight discrepancies are shown between front row cascade and rear row cascade zone

IV. Conclusions

The FA method developed by Chen et al. for the two-dimensional Navier-Stokes equations and energy equation are further developed to study turbulent flow in the general curvilinear coordinate system. The incompressible, steady and turbulent flow through the single and tandem cascade of airfoils are simulated using the FA method. The $k-\epsilon$ turbulent model and wall function are used in the present study. The comparison between the calculation results and the experimental data shown good predictions of the surface pressure distribution. Although further study may be required, the results here are quite encouraging.

Reference

1. G.C. Wu, B.N. Zhuang, B.H. Guo, Experimental Investigation of Tandem Blade Cascades with Double-Circular ARC Profiles, ASME 85-IGT-94.
2. G.C. Wu, Q. Feng, Optimization of the Front and Rear Blade Rows of a Tandem

Blade Cascade, 1987 Tokyo International Gas Turbine Congress, 87-TOKYO-IGTC-19.

3. W.E. Spralin, Flow through Cascades in Tandem, NACA TN2393, 1951.
4. A.A. Mikolajczak, et al., Flow through Cascades of slotted Compressor Blades, Trans. ASME, J. Eng. Power, Jan. 1970.
5. N.L. Sanger, Analytical Study of the Effects of Geometric Changes on the Flow Characteristics of Tandem Blades Compressor Stators, NACA TN D-6264, 1971.
6. K. Bammert, H. Beelte, Investigation of an Axial Flow Compressor with Tandem Cascades, ASME Paper 80-GT-39, Mar. 1980.
7. C.J. Chen, P.Li, The Finite Analytic Method for Steady and Unsteady Heat Transfer Problem, ASME paper 80-HT-86, 1980.
8. S.V. Patankar, Numerical Heat Transfer and Fluid Flow, McGraw-Hill, New York 1980.
9. P.J. Roach, Computational Fluid Mechanics, Hermosa Publishers, 1972.
10. S.Yu. Tuann, M.D. Olson, A Transient Finite-Element Solution Method for Navier-Stokes Equations, Comput. Fluids, Vol.6, pp141-152, 1978.
11. C.J. Chen, et al., Finite Analytic Numerical Solution of Heat Transfer in Two-Dimensional Cavity Flow, Numerical Heat Transfer, Vol.4, pp. 179-197, 1981.
12. R.J. Sorenson, J.L. Steger, Simplified Clustering of Nonorthogonal Equations, NASA TM73252, 1977.
13. F. Richard, J.C. Emery, A Comparison of Typical National Gas Turbine Establishment and NACA Axial Flow Compressor Blade Section, NACA TN-3937, 1957.
14. D. Xu, G.C. Wu, Finite Analytic Solution of Turbulent Flow over an Airfoil, Proceedings of the Fifth International Conference held at Montreal, Canada, on 6th-10th July, 1987, also Numerical Methods in Laminar and Turbulent Flow, Vol. 5, Part 1.

Appendix

$$C_{p1} = E \cdot \exp(-Ah/C - Bk/D); \quad C_{p2} = E \cdot \exp(Ah/C - Bk/D)$$

$$C_{p3} = E \cdot \exp(-Ah/C + Bk/D); \quad C_{p4} = E \cdot \exp(Ah/C + Bk/D)$$

$$C_{p5} = EB \cdot \exp(Ah/C); \quad C_{p6} = EB \cdot \exp(-Ah/C);$$

$$C_{p7} = EA \cdot \exp(Bk/D); \quad C_{p8} = EA \cdot \exp(-Bk/D);$$

$$C_p = (Ah(C_{p1} + C_{p2} + C_{p3} - C_{p4} - C_{p5} - C_{p6})$$

$$+ Bk(C_{p7} + C_{p8} - C_{p9} - C_{p10} - C_{p11})) / (2A^2 + 2B^2)$$

$$E = (E_1 + E_2) / 2 - (Ah/C) \cdot \coth(Ah/C) \cdot E_1$$

$$- (Bk/D) \cdot \coth(Bk/D) \cdot E_2$$

$$EA = 2(Ah/C) \cdot \cosh(Ah/C) \cdot \coth(Ah/C) \cdot E_1$$

$$EB = 2(Bk/D) \cdot \cosh(Bk/D) \cdot \coth(Bk/D) \cdot E_2$$

$$E_1 + E_2 = 1 / (2 \cosh(Ah/C) \cdot \cosh(Bk/D))$$

$$E_1 = (D/C) \cdot (h/k) \cdot E_2 + (Ak \cdot \tanh(Bk/D) - Bk \cdot \tanh(Ah/C)) / (4(Bk/D) \cdot Ak \cdot \cosh(Ah/C))$$

$$\cosh(Bk/D)$$

$$E = \sum_{m=1}^{\infty} \frac{(-1)^m \sqrt{\lambda_{2m-1}} h}{\cosh(\mu_{2m-1} k)} \left((Ah/C)^2 + (\sqrt{\lambda_{2m-1}} h)^2 \right)$$

$$\lambda_m = (m\pi/2h)^2; \mu_m = (A^2/C + B^2/D + C\lambda_m); m = 1, 2, \dots$$

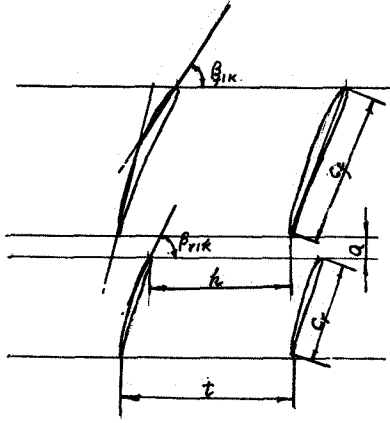


Fig. 1 Tandem cascade

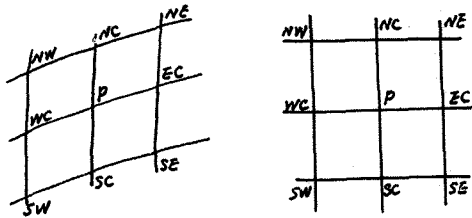


Fig. 2 Finite analytic element

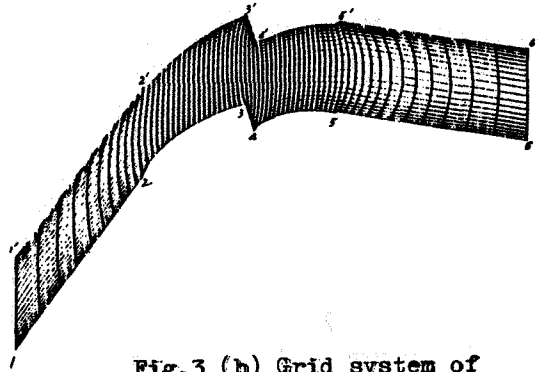


Fig. 3 (b) Grid system of tandem cascade

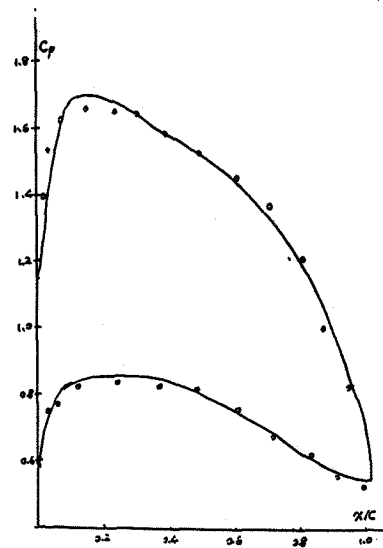


Fig. 4 Pressure distribution of single cascade

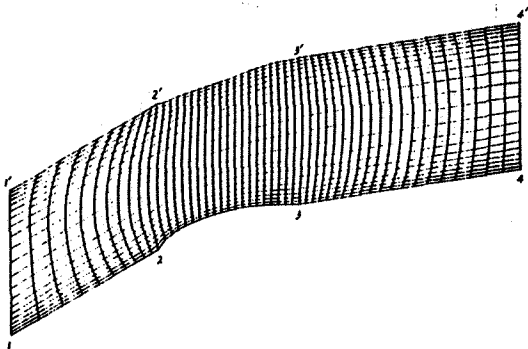


Fig. 3 (a) Grid system of single cascade

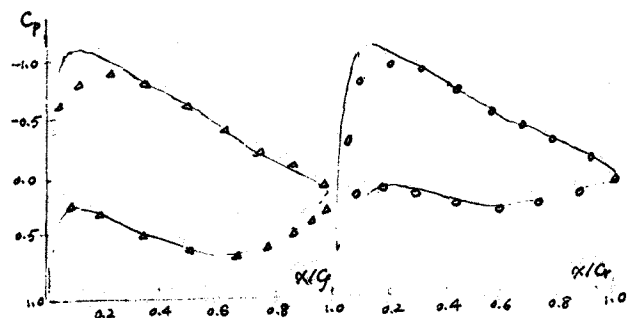


Fig. 5 Pressure distribution of tandem cascade